Published online 14 November 2008

Nucleic Acids Research, 2009, Vol. 37, No. 1 ***47–59***
doi:10.1093/nar/gkn901

Far upstream element binding protein 2 interacts with enterovirus 71 internal ribosomal entry site and negatively regulates viral translation

Jing-Yi Lin[1,2,3], Mei-Ling Li[1,5] and Shin-Ru Shih[1,2,3,4,*]

[1]Research Center for Emerging Viral Infections, [2]Department of Medical Biotechnology and Laboratory Science, [3]Graduate Program in Biomedical Science, Chang Gung University, Tao-Yuan, [4]Division of Biotechnology and Pharmaceutical Research, National Health Research Institutes, Zhunan, Taiwan and [5]Department of Molecular Genetics, Microbiology and Immunology, UMDNJ-Robert Wood Johnson Medical School, Piscataway, NJ, USA

Received July 28, 2008; Revised October 25, 2008; Accepted October 27, 2008

ABSTRACT

An internal ribosomal entry site (IRES) that directs the initiation of viral protein translation is a potential drug target for enterovirus 71 (EV71). Regulation of internal initiation requires the interaction of IRES *trans*-acting factors (ITAFs) with the internal ribosomal entry site. Biotinylated RNA-affinity chromatography and proteomic approaches were employed to identify far upstream element (FUSE) binding protein 2 (FBP2) as an ITAF for EV71. The interactions of FBP2 with EV71 IRES were confirmed by competition assay and by mapping the association sites in both viral IRES and FBP2 protein. During EV71 infection, FBP2 was enriched in cytoplasm where viral replication occurs, whereas FBP2 was localized in the nucleus in mock-infected cells. The synthesis of viral proteins increased in FBP2-knockdown cells that were infected by EV71. IRES activity in FBP2-knockdown cells exceeded that in the negative control (NC) siRNA-treated cells. On the other hand, IRES activity decreased when FBP2 was overexpressed in the cells. Results of this study suggest that FBP2 is a novel ITAF that interacts with EV71 IRES and negatively regulates viral translation.

INTRODUCTION

Enterovirus 71 (EV71), a positive-stranded RNA virus of the *Picornaviridae* family, poses a persistent global public health problem. EV71 presents most frequently as a child herpangina or exanthema, known as hand, foot and mouth disease (HFMD). However, acute EV71 infection is also associated with severe neurological complications with significant mortality. Children under 5-year-old are particularly susceptible to the most severe forms of EV71-associated neurological complications, including aseptic meningitis, brainstem and/or cerebellar encephalitis, myocarditis, acute flaccid paralysis and rapid fatal pulmonary edema and hemorrhage (1). Such presentations as well as a poliomyelitis-like syndrome have been observed during outbreaks in Taiwan, mainland China, Malaysia, Singapore, western Australia, the United States and Europe (2–8). With the emergence of EV71 worldwide as the major causative agent of HFMD fatalities in recent years, and in the absence of any effective anti-enteroviral therapy, a need clearly exists to find a specific anti-EV71 agent. The internal ribosomal entry site (IRES) of EV71 is a good target for the development of an antiviral agent because viral replication can be restricted by inhibiting IRES-mediated viral translation.

A 40S ribosomal subunit recognizes a sequence, RNA structure or ribonucleoprotein complex within the IRES, and initiation occurs at the authentic start codon of the picornaviral RNA. During infection by poliovirus (PV), human rhinovirus (HRV), EV71 or coxsackievirus, the viral proteases 3C and 2A cleave cellular proteins, including the translation initiation factor eIF4G, causing rapid termination of the host cap-dependent translation (9–12). The IRES-mediated initiation of translation allows viral RNA translation while host cell translation is shut down during infection. IRES-dependent translation depends on both canonical translation initiation factors and IRES-specific *trans*-acting factors (ITAFs). These ITAFs interact with various IRES elements to regulate their activities by affecting ribosome recruitment or modifying the structure of the IRES itself. Several proteins that modulate the picornaviral IRES function as ITAFs have been identified: these include polypyrimidine tract binding protein (PTB), poly(rC)-binding protein 1 (PCBP1), poly(rC)-binding

*To whom correspondence should be addressed. Tel: +886 3 2118800 (ext. 5497); Fax: +886 3 2118174; Email: srshih@mail.cgu.edu.tw

protein 2 (PCBP2), autoantigen La, upstream N-ras protein (Unr) and ITAF$_{45}$ (13–16).

Only a few investigations have described the IRES for EV71 (12,17), and the ITAFs for EV71 have not been intensively studied. This work reports the use of the biotinylated RNA-protein pull-down approach followed by matrix-assisted laser desorption ionization/time-of-light mass spectrometer (MALDI-TOF) analysis, to identify 12 cellular proteins that are associated with EV71 5′ UTR which contains IRES in SF268 cells. Three of these—PTB, PCBP1 and PCBP2—shown have already been demonstrated to interact with the 5′ UTR of picornavirus (18–20). This investigation identifies FBP2 as one of the cellular proteins that is associated with the EV71 5′ UTR *in vitro* and *in vivo*. The interaction between FBP2 and EV71 5′ UTR was further confirmed by mapping the interaction regions in both viral RNA and FBP2 protein. The localization of FBP2 in EV71 infected-cells was examined and the role of FBP2 in viral translation was also investigated.

MATERIALS AND METHODS

Plasmid construction

The pT7-EV71 5′ UTR was constructed as follows: the 5′ UTR of EV71 was amplified by PCR from the EV71 full-length infectious cDNA clone (21) using EV71 5′-(GCCGGTAATACGACTCACTATAGGGAGATTA AAACAGCCTGTGGGT) and EV71 5′-(CATGTTTGA TTGTGTTGAGGGTCAAAAT) primers that contained the T7 promoter, and was cloned into pCRII-TOPO vector by TA cloning (Invitrogen, California, USA).

pCMV-tag2B-KSRP (a gift from Dr. Roberto Gherzi, Istituto Nazionale per la Ricerca sul Cancro, Italy) was utilized to construct various truncated forms of flag-tagged KH motifs of FBP2, and fragments were amplified by PCR using a 5′ primer that contained an EcoR I site and a 3′ primer that contained a Xho I site. PCR products were subcloned between the EcoR I and Xho I sites of pCMV-tag2B vector.

The pRHF was constructed as follows: Renilla Luciferase gene (R) was inserted in EcoR I site of pTriEx-4; Firefly Luciferase gene (F) was inserted in Xho I of pTriEx-4; A hairpin (H) was inserted downstream of the Renilla Luciferase gene to prevent ribosome read-through. A dicistronic reporter plasmid, pRHF–EV71-5′ UTR, containing EV71 5′ UTR between Renilla and Firefly luciferase was constructed by insert a Not I–EV71-5′ UTR–Not I fragment to pRHF.

Preparation of SK-N-MC, SF268 and RD cell extracts

SK-N-MC (human neuroblastoma), SF268 (human glioblastoma) and RD (human embryonal rhabdomyosarcoma) cells were grown in Dulbecco's Modified Eagle medium (GIBCO, California, USA) supplemented with 10% fetal bovine serum. Upon confluence, cells were pelleted, washed three times with cold PBS, resuspended in CHAPS buffer (10 mM Tris–HCl pH 7.4, 1 mM $MgCl_2$, 1 mM EGTA, 0.5% CHAPS, 10% glycerol, 0.1 mM PMSF, 5 mM 2-ME), and then incubated on ice for 30 min for swelling. Cell lysates were isolated by centrifugation at 10 000*g* for 10 min at 4°C, and the supernatants were collected for further analysis. The concentrations of the proteins in the cell extracts were determined using the Bio-Rad protein assay (Bio-Rad, Hercules, CA).

In vitro transcription

The T7 promoter–EV71-5′ UTR fragment that was flanked by EcoR I sites was excised from the pCRII-TOPO vector. RNA transcripts were synthesized using the MEGAscript T7 kit (Ambion, Texas, USA), according to the protocol provided by the manufacturer. Biotinylated RNA was synthesized in a 20 µl MEGAscript transcription reaction mixture by the addition of 1.25 µl of 20 mM biotinylated UTP, Bio-16-UTP, which is a substrate for SP6, T3 and T7 RNA polymerases and can replace UTP in the *in vitro* transcription for RNA labeling (Roche, Penzberg, Germany). Synthesized RNAs were purified using the RNeasy Protect Mini Kit (Nobel, Hilden, Germany) and analyzed on 1% agarose gels.

Isolation of proteins associated with EV71 5′ UTR RNA sequences by affinity binding to biotinylated RNA

A reaction mixture that contained 200 µg of cell extracts and 12.5 pmol of a biotinylated EV71 5′ UTR RNA probe was made. The mixture (with a final volume of 100 µl), which contained 5 mM HEPES pH 7.1, 40 mM KCl, 0.1 mM EDTA, 2 mM $MgCl_2$, 2 mM dithiothreitol, 1 unit RNasin and 0.25 mg/ml heparin (RNA mobility shift buffer), was incubated for 15 min at 30°C, and then added to 400 µl of Streptavidin MagneSphere Paramagnetic Particles (Promega, Wisconsin, USA) for binding for 10 min at room temperature. The protein–RNA complexes were washed five times with the RNA mobility shift buffer without heparin. After the last wash, 30 µl of 2 × SDS–PAGE sample buffer was added to the beads, which were then incubated for 10 min at room temperature to dissociate the proteins from the RNA. The sample that contained the eluted proteins was then boiled, subjected to 8–16% SDS–PAGE, and further visualized by silver staining or western blotting. Proteins bands were excised and identified by in-gel trypsin digestion and analyzed by Bruker Ultraflex MALDI-TOF mass spectrometry.

Database-searching algorithm

After the masses that were derived from the standards, trypsin, matrix and keratins had been removed, the monoisotopic mass lists for each protonated peptide were used to search the database. Mass lists were exported to the Biotool 2.0 software package to perform peptide mass fingerprinting via Mascot (http://www.matrixscience.com) algorithm scoring to identify proteins.

Western blot analysis

PVDF membranes were blocked with Tris-buffered saline/0.1% (vol/vol) Tween 20 that contained 5% non-fat dry milk and probed with the indicated antibodies. The antibodies against FBP2 (1:200; Santa Cruz Biotechnology,

Santa Cruz, CA, USA), PTB (1:500; Santa Cruz Biotechnology, Santa Cruz, CA, USA), flag (1:2000; SIGMA, Missouri, USA) and actin (1:5000; Chemicon, USA) were used. After washing, the membrane was incubated with HRP-conjugated anti-mouse antibody or HRP-congugated anti-goat antibody, as appropriate (diluted 1:5000). HRP was detected using the Western Lightning Chemiluminescence Kit, following the manufacturer's protocol (Amersham Pharmacia, Freiburg, Germany).

Coimmunoprecipitation and RT-PCR

Cell extracts from EV71-infected RD cells for use in coimmunoprecipitation assays were prepared at 6 h post-infection. Lysates were precleared by incubation on ice for 1 h with protein A-agarose (50% in lysis buffer) that was bound to non-specific antibody. Non-specific complexes were pelleted by centrifugation at 10 000*g* at 4°C for 10 min. The supernatants were removed and used in the immunoprecipitation assay. Next, 100 µl of precleared lysate was diluted with 450 µl of lysis buffer and then added to 15 µl of flag antibody, before incubation on ice for 2 h. Prewashed protein A-agarose [100 µl in PBS (50:50)] was added to each sample, which was then incubated on ice for an additional hour. Immune complexes were pelleted by centrifugation at 1000*g* at 4°C for 5 min and washed three times with lysis buffer. Each pellet [or 100 µl of precleared lysate (total RNA)] was resuspended in 400 µl of proteinase K buffer [100 mM Tris–HCl (pH 7.5), 12.5 mM EDTA, 150 mM NaCl, 1% SDS] and incubated with 100 µg of predigested proteinase K for 30 min at 37°C. RNA was extracted with phenol-chloroform, precipitated in ethanol at –20°C for 1 h, washed in 70% ethanol, dried and resuspended in 20 µl DEPC H_2O. RT-PCR was performed using a Reverse-iT One-Step TR-PCR kit (ABgene, Surry, UK) and either primers specific to EV71 5′ UTR or primers specific to ribosomal protein S16 (GCGCGGTGAGGTTGTCTAGTC and GAGTTTTG AGTCACGATGGGC).

Fluorescence microscopic analysis

RD cells grown on glass cover slips were infected with EV71 for 1 h at an MOI of 40. After 6 h post-infection, the culture medium was removed, and the cells washed three times with PBS. The cells on the coverslip were fixed with 3.7% (wt/vol.) formaldehyde at room temperature for 20 min. After being washed three times with PBS, the cells on the coverslip were permeabilized in 0.5% Triton X-100 at room temperature for 5 min and washed again three times with PBS. For flag and EV71 3A immunostaining, the samples were blocked in solution [PBS, containing 5% bovine serum albumin (BSA)] for 60 min at room temperature and then incubated with anti-flag antibody (1:200) for 1.5 h at room temperature and washed three times with PBS. The samples were then reacted with FITC (Fluorescein Isothiocyanate)-conjugated goat anti-mouse IgG and rhodamine [tetramethyl rhodamine isothiocyanate (TRITC)]-conjugated goat anti-rabbit IgG (Jackson ImmunoResearch Laboratories, Inc.) for 1 h at room temperature. After being washed with PBS, the samples were treated with Hoechst 33258 for 15 min at room temperature and washed again with PBS three times. Finally, the coverslips with adhering cells were placed on a glass slide and sealed with transparent nail polish. The images were captured by confocal laser scanning microscopy (ZEISS LSM510 META).

Virus infections and metabolic radiolabeling

Forty-eight hours after siRNA transfection, 2×10^5 RD cells were seeded into 12-well plates and incubated at 37°C for 24 h. The cells were then infected with EV71 at a multiplicity of infection of 40 PFU per cell. Virus was adsorbed at room temperature for 1 h. The medium was then replaced with methionine-free DMEM, and incubation was continued at 35°C. At various times post-infection, the medium was replaced with medium with ^{35}S-Met labeling (50 µCi/ml). After 1 h of labeling, the cell monolayers were washed with PBS and lysed with lysis buffer. Cell lysates were isolated by centrifugation at 10 000*g* for 10 min at 4°C, and the supernatants were collected for further analysis. Radiolabeled proteins were resolved by SDS–PAGE (12% gels), transferred to a PVDF membrane, and detected by autoradiography. The same membrane was used for Western blotting. The sequence of FBP2 siRNA is 5′-CACAUUCGUAUUCUGAGAUCC GUCC-3′ (Invitrogen, KHSRP-HSS112554); and the sequence of NC siRNA is 5′-AACUGGGUAAGCGGG CGCAAAUU-3′.

Dicistronic or monocistronic expression assay

For dicistronic expression assay, RD cells were firstly transfected with either FBP2 siRNA or pFBP2/FLAG. After 3 days, dicistronic construct pRHF or pRHF–EV71-5′UTR and siRNA duplexes were cotransfected into RD cells with siRNA duplex. After 2 days, cell extracts were prepared in passive buffer (Promega) and assayed for Renilla luciferase (RLuc) and Firefly luciferase (FLuc) activity in a Lumat LB9507 bioluminometer using a dual-luciferase reporter assay (Promega) according to the manufacturer's instructions. For western blotting experiment, cell lysates were incubated at 95°C for 5 min, and an equal amount of proteins was resolved on sodium dodecyl sulfate (SDS)–12% polyacrylamide gels. For capped dicistronic mRNA containing a poly(A) tail reporter or monocistronic RNA reporter assay, RD cells transfected with either FBP2 siRNA or FBP2/FLAG were grown for 3 days and then transfected with RNA. After 6-h post-transfection, cells were harvested, lysed and western blotted for FBP2, FBP2/FLAG and actin.

Evaluating RNA replication by slot blotting

RD cells were transfected with FBP2 and NC (negative control) siRNA for 48 h, and then trypsinzed and counted. About 2×10^5 cells were seeded into 12-well plates. After 24 h, the cells were then challenged with EV71 (4643/TW/1998) at a multiplicity of infection (MOI) of 40 per cell and were harvested at 1, 2, 3, 4, 5, 6, 7, 8 and 9 h post-infection. RNA were extracted and dissolved in a solution of formaldehyde and 20× SSC for 30 min at 60°C. The reaction was then loaded onto a nitrocellulose sheet in the

slot-blot manifold. After two washings, the nitrocellulose was removed, air-dried and crosslinked in a Stratalinker at 200 J for 9 min. The nitrocellulose was prehybridized at 68°C for 30 min in DIG Easy Hyb (Roche, Germany). DIG-labeled RNA probes, specific for either the genome or the antigenome were produced using DIG Northern Starter kit (Roche, Germany). Following the addition of the probes at 100 ng probe/ml, the blots were incubated at 68°C for 16 h. Following the hybridization, the membrane was immediately submerged in the tray that contained Low Stringency Buffer (2 × SSC with 0.1% SDS) at room temperature for 5 min with shaking. Then, the blot was incubated twice (2 × 15 min, with shaking) in High Stringency Buffer (0.1 × SSC with 0.1% SDS) at 68°C. The membrane was then incubated with wash buffer for 2 min at room temperature with shaking. After the membrane had been blocked with blocking solution for 30 min, it was incubated with the anti-Digoxigenin-AP antibody solution for 30 min and then washed twice with washing buffer (0.1 M Maleic acid, 0.15 M NaCl; pH 7.5; 0.3% (v/v) Tween 20). It was then equilibrated for 5 min in 20 ml detection buffer (0.1 M Tris–HCl, 0.1 M NaCl, pH 9.5). Finally, the chemiluminescent substrate (CDP-Star) was added to the membrane and the membrane was exposed to a Kodak film.

Expression and purification of recombinant PTB protein

PTB cDNA that was derived from SF268 cellular mRNA was cloned into PET30a, a prokaryotic expression vector that contained a histidine tag (Novagen Inc., Madison, Wisc., USA), via restriction sites EcoR I and Hind III. After the constructed plasmid (pET30a/PTB) was introduced into a competent cell *E. coli* BL21 (DE3 pLysS), His-PTB fusion protein expression was induced with 40 μM isopropyl β-D-thiogalactopyranoside (IPTG) at 37°C for 2 h. The recombinant protein was then purified using a HisTrap™ kit (Pharmacia, NJ, USA). The concentration of the protein was measured by Bio-Rad protein assay (Bio-Rad).

RESULTS

FBP2 associates with EV71 5′ UTR

To gain a better understanding of the function of EV71 5′ UTR that contains IRES, biontinylated RNA-affinity chromatography, followed by matrix-assisted laser desorption ionization/time-of-flight mass spectrometry (MALDI-TOF MS), was performed to isolate and identify cellular proteins that associate with EV71 5′ UTR RNA. The full-length sequence of EV71 5′ UTR that retains full activity and maintains the correct secondary structure of IRES was employed. Streptavidin beads were used to capture biotinylated EV71 5′ UTR bound to cellular proteins. Figure 1A presents the results of a biotinylated RNA-affinity chromatography assay. Lane 1 presents the control without any RNA. The patterns of the pull-down protein bands of the control and SF268 cell lysates that were incubated with biotin-16-UTP (lane 2) were identical. When the cell lysates were reacted with biotinylated EV71 5′ UTR, at least 16 bands with distinct sizes (lane 4) were present in the SF268 cells, suggesting that these proteins may be associated specifically with the EV71 5′ UTR. In the reactions of cell extracts with non-biotinylated EV71 5′ UTR, the patterns of the protein bands (lane 3) were identical to those of the controls.

The protein bands that were specifically associated with biotinylated EV71 5′ UTR RNA (lane 4) in Figure 1A were then extracted, digested with trypsin, and subjected to MALDI-TOF MS analysis. Table 1 presents these proteins with their accession numbers obtained from the protein database. Sixteen bands, presenting 12 proteins, were identified. They comprised three known ITAFs that interacted with the IRES of picornavirus. They were polypyrimidine tract-binding protein (PTB, bands 11-1 and 11-2), poly(C) binding protein 2 (PCBP2, bands 12 and 13) and poly(C) binding protein 1 (PCBP1, band 14).

One novel protein far upstream element binding protein 2 (FBP2, band 5) was chosen and its functions on EV71 5′ UTR were investigated. To confirm the interaction between the EV71 5′ UTR and FBP2, the RNA-protein pull down assay was performed as described, and different amounts of non-biotinylated EV71 5′ UTR or yeast tRNA was added for competition assay. As revealed by Figure 1B, this interaction was out-competed by non-biotinylated EV71 5′ UTR (lanes 3, 4 and 5) but not by yeast tRNA (lanes 8, 9 and 10), demonstrating that FBP2 does not interact non-specifically with any RNA sequence.

The above experiments were conducted in SF268 cells. To know whether the interactions also occurred in other cells, RNA-protein pull down assay was performed in various cell extracts. As shown in Figure 1C, the association of FBP2 with biotinylated EV71 5′ UTR occurred not only in neural cells lines, SK-N-MC (lane 5) and SF268 cells (lane 10), but also in the non-neural cell line, RD cells (lane 15). The association of FBP2 with EV71 5′ UTR is likely to be a common interaction amongst different cell lines.

Interaction regions in viral RNA and in FBP2 protein

EV71 5′ UTR contains cloverleaf and IRES structures, verifying and elucidating in greater detail the interaction between EV71 5′ UTR and FBP2, enabling the binding regions in both viral RNA and FBP2 protein to be further mapped. Figure 2A presents the potential secondary structure of EV71 5′ UTR as predicted by M-FOLD. Various truncated forms of viral RNAs, as displayed in Figure 2B, were synthesized by *in vitro* transcription and labeled with biotin. The aforementioned RNA protein pull-down assay was performed, and the streptavidin beads were used to capture the biotinylated viral RNA and its associated cellular proteins from SF268 cells. Western blot was then conducted to measure the interactions of FBP2. As presented in Figure 2B, biotinylated probes 1–167 (lane 4), 91–228 (lane 6), 91–636 (lane 12), 91–745 (lane 14), 453–636 (lane 20), 453–745 (lane 22) and 566–745 (lane 24) pulled down FBP2 from SF268 cell lysates, while the other probes did not. The results suggest that FBP2 may interact with the nt 1–167 (stem-loop I-II), 91–228 (stem-loop II-III) and 566–745 (stem-loop VI and spaer region) regions in EV71 5′ UTR.

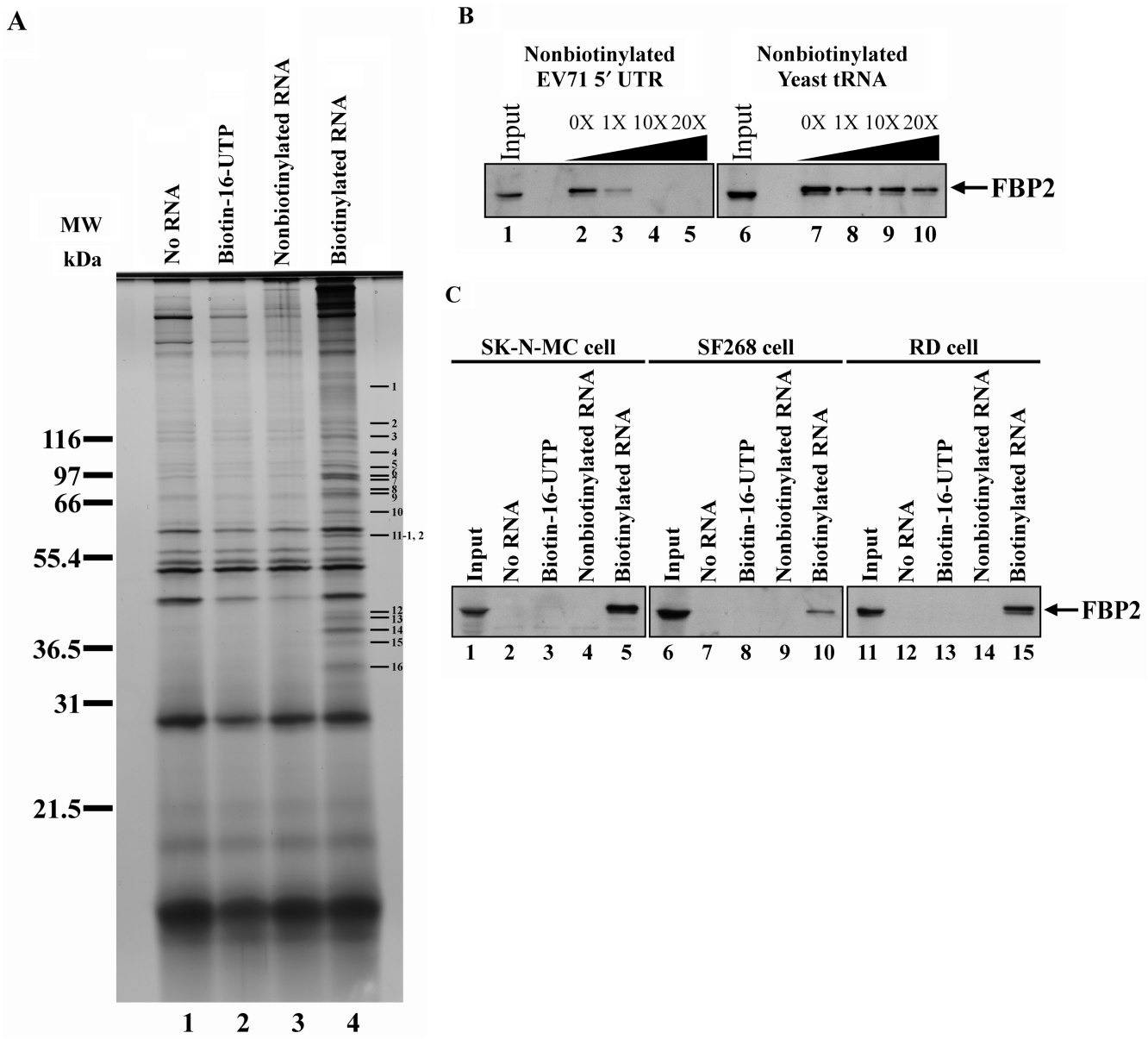

Figure 1. Identification of interaction of FBP2 with enterovirus 71 5′ untranslated region (EV71 5′ UTR). (**A**) Identification of cellular proteins associated with EV71 5′ UTR. RNA-protein pull-down experiments were performed as described in Materials and methods section. EV71 5′ UTR was labeled with biotin and incubated with SF268 cell lysate (200 μg) for 15 min at 30°C. Streptavidin was then used to pull down biotin-labeled RNA (EV71 5′ UTR) and its associated cellular proteins (lane 4). After they had been washed and dissociated from RNA, the eluted proteins were boiled and subjected to SDS–PAGE (8–16% gradient gel). Silver staining was applied for visualization. In the negative controls, no RNA was added to the reaction for lane 1; biotin-16-UTP was added to the reaction for lane 2; non-biotinylated RNA was added to the reaction for lane 3. A comparison with the control lanes 1–3 revealed that some protein bands appeared only in lane 4. Those bands were excised, digested in gel, and analyzed by MALDI-TOF. (**B**) Specific association of FBP2 with EV71 5′ UTR was confirmed by western blot and competition assay. The pull-down assay that was displayed in Figure 1A was performed here. The eluted proteins were also subjected to SDS–PAGE (12%). Antibody against FBP2 was utilized in the western blot analysis. Various amounts of unlabeled RNA were added to compete with biotin-labeled EV71 5′ UTR in interacting with FBP2. Lanes 1 and 6 contained cell lysate (200 μg) only. Unlabeled EV71 5′ UTR was used in the competition assay (lanes 3–5), and unlableled yeast tRNA was utilized (lanes 8–10). (**C**) EV71 5′ UTR associates with FBP2 in the various cell lines. The 100% inputs of different cell extracts only are shown in lanes 1, 6 and 11. SK-N-MC, SF268 and RD cell extracts were incubated in the absence of RNA (lanes 2, 7 and 12) or in the presence of biotin-16-UTP (lanes 3, 8 and 13), non-biotinylated full-length EV71 5′ UTR (lanes 4, 9 and 14) or biotinylated full-length EV71 5′ UTR (lanes 5, 10 and 15). After the beads were washed, bound proteins were resolved using 12% SDS–PAGE. FBP2 protein was visualized by immunoblot analysis with anti-FBP2 proteins antibody.

FBP2 contains a proline/glycine-rich N-terminus with a nuclear localization signal, a central region with four KH-type RNA-binding domains and an unusual C terminus rich in glutamine with four degenerate copies of the repeat DYTKAWEEYYKK. An attempt was made to identify the domains within FBP2 that are involved in the interaction with EV71 5′ UTR. Different truncated forms of DNA constructs were generated to express

Table 1. MALDI-TOF results for cellular proteins associated with EV71 5′ UTR

Number	NCBI	Match	Sequence Coverage (%)	Mass (Da)
1	Pro alpha (I) collagen	76045	13	139 571
2	Lrp protein	S57723	15	100 135
3	PTB-associated splicing factor, long form	A46302	24	76 216
4	Keratin	—	—	—
5	Fuse binding protein 2	Q92945	46	68 735
6	glycyl-tRNA synthetase	P41250	27	83 828
7	glycyl-tRNA synthetase	P41250	23	83 828
8	FUSE binding protein	Q12828	37	67 690
9	Keratin	—	—	—
10	Heterogeneous nuclear ribonucleoprotein K	P61978	35	50 996
11-1	Polypyrimidine tract-binding protein PTB-1	Q9BUQ0	35	59 767
11-2	Polypyrimidine tract-binding protein PTB-2	S23016	35	59 172
12	poly(rC) binding protein 2	Q6IPF4	40	38 955
13	poly(rC) binding protein 2	Q6IPF4	41	38 955
14	poly(rC) binding protein 1	S58529	21	37 987
15	Keratin	—	—	—
16	Heterogeneous nuclear ribonucleoprotein A1	ROA1_HUMAN	47	38 805

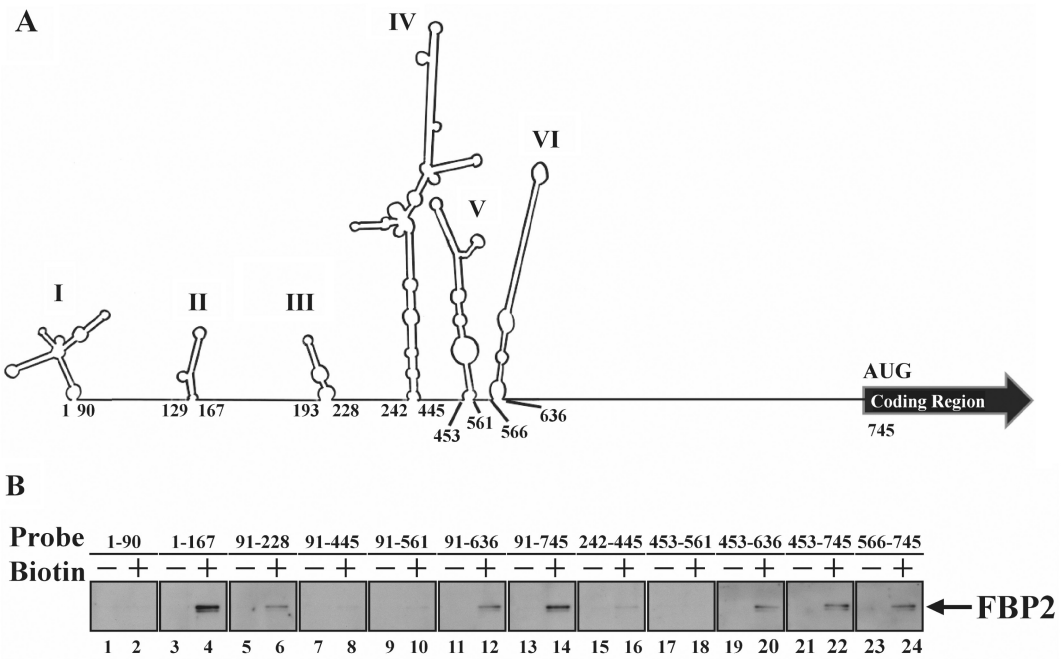

Figure 2. Interaction regions in EV71 5′ UTR for FBP2. (**A**) Predicted RNA secondary structure for 5′ UTR. M-FOLD software was utilized to predict the RNA secondary structure. The first and the last nucleotides in each stem-loop are numbered as indicated. (**B**) Map of regions of interaction in RNA. Various truncated forms of RNA, as indicated, were transcribed *in vitro* and biotinylated. SF268 cell lysates were incubated with those biotin-labeled RNAs (lanes 2, 4, 6, 8, 10, 12, 14, 16, 18, 20, 22 and 24). Non-biotinylated RNA probes were as controls (lanes 1, 3, 5, 7, 9, 11, 13, 15, 17, 19, 21 and 23). After being pulled down by streptavidin beads, the protein complex was dissolved in the SDS–PAGE as described above. Western blot was then applied to detect FBP2 in the pull-down complex.

FBP2 fused with the FLAG (Figure 3A) and their ability to interact with EV71 5′ UTR was tested by RNA-protein pull down assay. These plasmids were transfected individually into RD cells and the cell lysates were utilized in RNA-protein pull down experiments. The expressions of FBP2 (lane 1) and the truncated forms (lanes 4, 7, 10 and 13) were visualized by western blot using anti-flag antibody (Figure 3B). Streptavidin beads captured biotinylated EV71 5′ UTR and its associated full-length FBP2, as well as two truncated forms, FBP2-KH_{1-4} and FBP2-KH_{2-4}, but not FBP2-KH_{1-3} and FBP2-KH_{3-4}. These results suggest that FBP2 may interact with EV71 5′ UTR through a region that contains at least KH2 and KH4 RNA-binding domains.

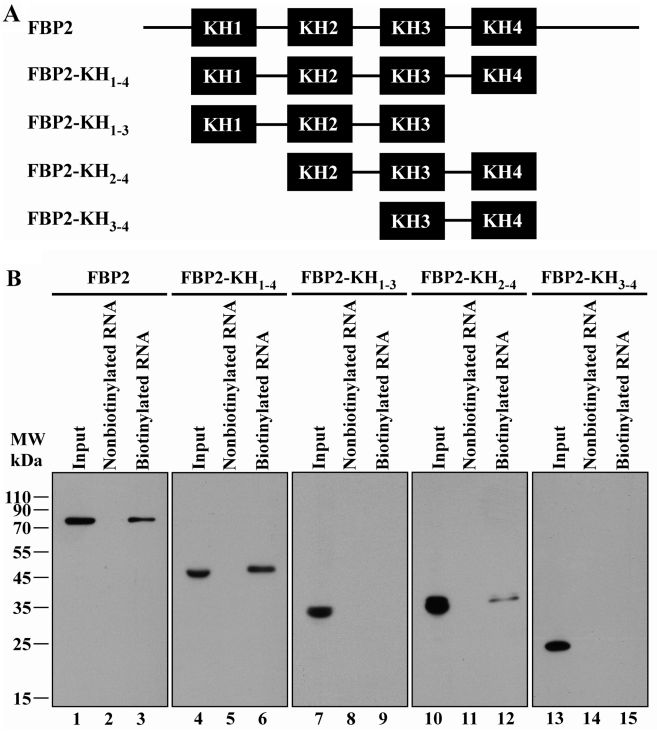

Figure 3. Interaction domains in FBP2 protein for EV71 5′ UTR. (**A**) Schematic diagram of FBP2 and various truncated mutants. The KH domains are indicated by black boxes. Four truncated forms, FBP2-KH_{1-4}, FBP2-KH_{1-3}, FBP2-KH_{2-4} and FBP2-KH_{3-4} were generated and fused with Flag at their N terminals. (**B**) Expressions of truncated forms of FBP2 in RD cells and mapping interaction regions in FBP2. Plasmids that carried wild-type (lane 1) or various truncated forms of FBP2 (lanes 4, 7, 10 and 13) were transfected into RD cells. Western blot using anti-Flag antibody was employed to examine protein expression. Cell extracts from transfected cells were collected 48 h post-transfection and then incubated with biotinylated RNA (EV71 5′ UTR). Streptavidin beads were used in the pull-down assay and the complex was dissolved for SDS–PAGE analysis. The amount of 'input' was exactly the same (100%) as the total amount of material used in the binding reaction.

EV71 infection redistributes FBP2 to different subcellular compartments

FBP2 is localized in the nucleus, while EV71 replication occurs in the cytoplasm. How FBP2 in the nucleus associates with EV71 5′ UTR is unclear. To characterize further the cellular localization of FBP2 in EV71-infected cells, their subcellular localization after EV71 infection was compared with that after mock infection by fluorescence microscopy. For this purpose, DNA constructs were generated to express FBP2 fused with the flag. These constructs were transfected into RD cells for 2 days and then the transfected cells were infected by EV71 at 40 MOI; the subcellular distribution of the fusion proteins was analyzed by fluorescence confocal microscopy at 6-h post-infection. In the absence of EV71 infection, FBP2 protein is mainly localized in the nucleus of the cells (Figure 4A-4). However, EV71 infection redistributes FBP2 to the cytoplasm (Figure 4A-9). Staining with antibody against viral 3A protein identified the EV71-infected cells. Hoechst 33258 was the dye specific for the nucleus. The data indicate that FBP2 is being relocalized from the nucleus to the cytoplasm or retained in the cytoplasm during EV71 infection.

FBP2 associates with EV71 5′ UTR in EV71 infection

FBP2 was determined to redistribute to the cytoplasm upon EV71 infection, and then whether the FBP2 associates with EV71 5′ UTR in EV71 infected-cells was examined. FBP2/FLAG was overexpressed in RD cells, which were then challenged by EV71 at 40 MOI. After 6, 7 and 8 h EV71 post-infection, the cells were lyzed and the RNA-protein complexes were immunoprecipitated by antibody specific to flag that fused with FBP2 or HA (as a negative control). RNA was isolated from these immunoprecipitates and then subjected to the RT-PCR reaction using with primers specific to either EV71 5′ UTR or ribosomal protein S16 (RPS16, as a control). At 6, 7 and

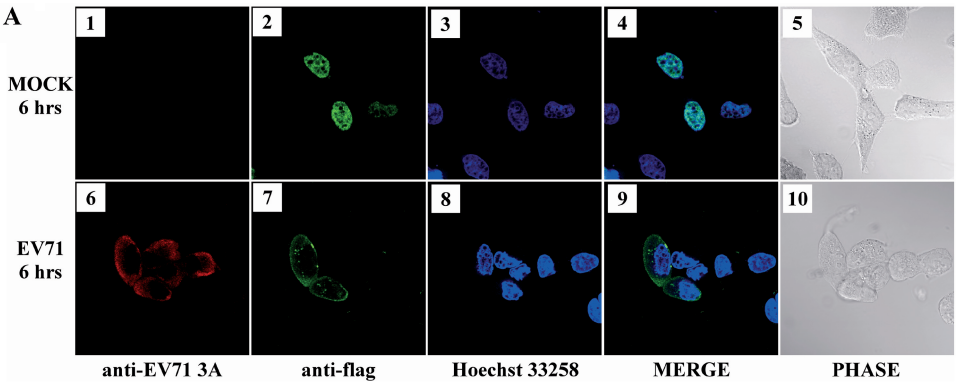

Figure 4. FBP2 localized to cytoplasm and associated with EV71 5′ UTR in EV71-infected cells. (**A**) Effect of EV71 infection on FBP2 localization. RD cells were transfected with pFlag-CMV2-FBP2. After 2 days, transfected cells were mock-infected or infected with EV71 at 40 MOI for 6 h and then fixed and stained with antibodies directed against Flag and viral protein 3A. Panels 1 and 6 show cells examined with a Rhodamin filter; panels 2 and 7 show cells examined with a FITC filter; panels 3 and 8 present Hoechst 33258 staining of the same field with a 4′, 6′-diamidino-2-phenylindole (DAPI) filter; panels 4 and 9 show merged FITC and Hoechst images and panels 5 and 10 present the phase of the cells.

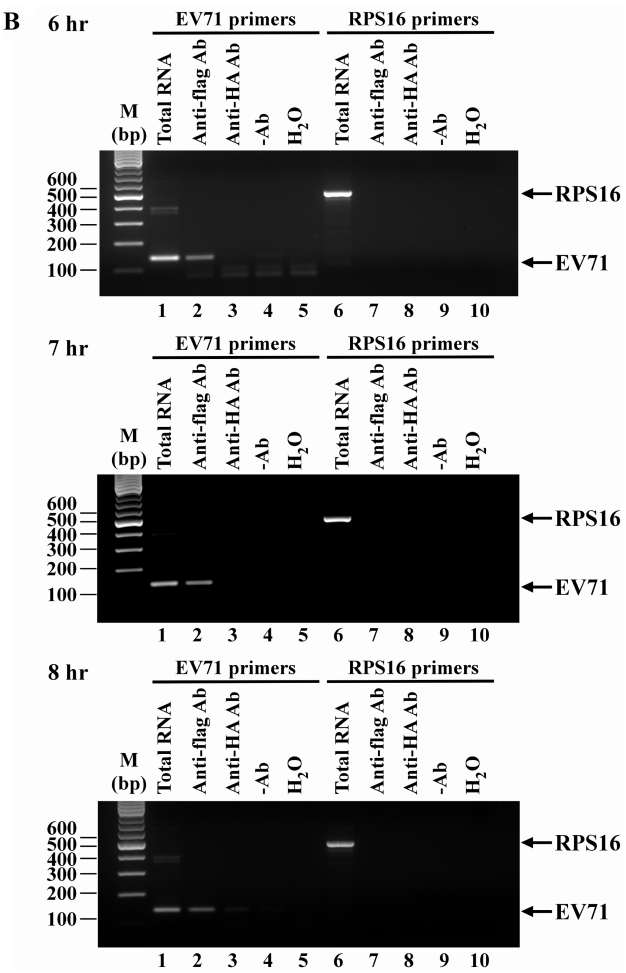

Figure 4. Continued.
(**B**) EV71 5′ UTR RNA was pulled down with FBP2 from EV71-infected cell extracts. RD cells were transfected with pFlag-CMV2-FBP2. After 2 days, transfected cells were infected by EV71 at 40 MOI. The cell extract was collected 6 h post-infection. Anti-Flag antibody was used in the immunoprecipitation assay. Following washing and dissociation, the RNA was extracted and subjected to the RT-PCR reaction using primers that were specific to either EV71 5′ UTR or ribosomal protein S16 (RPS16). Cell lysate without immunoprecipitation was used for RNA extraction (lanes 1 and 6) as an RT-PCR control. Anti-Flag antibody was incubated with 200 µg infected cell lysate and then underwent RNA extraction and RT-PCR analysis (lanes 2 and 7). The same reaction with anti-HA antibody or without antibody was performed used as a negative control (lanes 3, 4, 8 and 9). H_2O as a template was an RT-PCR negative control (lanes 5 and 10). FBP2 protein binds to the EV71 5′ UTR RNA but not to the control RNA (RPS16).

8 h post-infection, Immunoprecipitation with flag antibodies coprecipitated EV71 5′ UTR (Figure 4B, lane 2), but not the control RNA (RPS16) (Figure 4B, lane 7), confirming that FBP2 associates with EV71 5′ UTR in EV71 infected cells. No specific band that represented EV71 5′ UTR or RPS16 was detected when the reaction proceeded with anti-HA antibody (Figure 4B, lanes 3 and 8) or without antibody (Figure 4B, lanes 4 and 9). H_2O as a template was an RT-PCR negative control (Figure 4B, lanes 5 and 10). The results of Figures 1 and 4B together demonstrate that FBP2 associates with EV71 5′ UTR both *in vivo* and *in vitro*.

Viral protein synthesis was increased upon knockdown of FBP2 and decreased upon over-expression of FBP2

FBP2 was mapped to interact within the regions of IRES which is reported to participate in viral protein translation. This investigation further examined the synthesis of viral protein in knocked-down FBP2 or over-expressed FBP2. The RNA interference (RNAi) method was applied to investigate the dependency of EV71 translation on FBP2 *in vivo*. To examine the effect of FBP2 knockdown on EV71 translation, RD cells were transfected with siRNA (NC as negative control or siRNA against FBP2) and then infected with EV71 at 40 MOI. The cells were pulse-labeled with [^{35}S] methionine at various times post-infection, and extracts were analyzed by SDS–12% PAGE. Infection with EV71 inhibited the synthesis of host cell protein (Figure 5A and C), as expected. The results showed that viral protein synthesis in FBP2-depleted cells exceeded that in NC siRNA-treated cells (Figure 5A); whereas viral protein synthesis in FBP2-overexpressed cells was less than that of control (transfected with FLAG vector only) cells (Figure 5C). Figure 5B displays knockdown efficiency of FBP2 and Figure 5D exhibits the over-expression of FBP2. The integrity of cellular protein, eIF4G that has been reportedly cleaved by viral 2A protease shortly after viral infection, was also monitored. This result reveals that FBP2 may participate in viral translation as a negative modulator.

FBP2 negatively regulates IRES-dependent translation of EV71

During EV71 infection, the IRES-mediated initiation of translation allows viral RNA translation. Whether the knockdown or over-expression of FBP2 has any effect on EV71 IRES activity was further examined. A dicistronic reporter plasmid was used to evaluate EV71 IRES activity (Figure 6A); translation of the first cistronic (Renilla luciferase, RLuc) is cap-dependent, whereas the translation of second cistronic (Firefly luciferase, FLuc) is dependent on EV71 IRES activity. Calculating the ratio of FLuc expression to RLuc expression yields the relative IRES activity. First, the siRNA duplex—either NC siRNA or siRNA against FBP2—was transfected to RD cells, and then the siRNA duplex and the dicistronic plasmid were co-transfected into RD cells after 72 h post-transfection. Cell lysates were collected and analyzed to determine RLuc and FLuc activity after 48 h post-transfection. Knockdown of endogenous FBP2 protein increases EV71 IRES activity to 135% ($P < 0.001$) of that of the NC control (Figure 6A, left). The lower panel of 6A presents the knockdown efficiency of FBP2. Moreover, RD cells were transiently transfected with a FLAG-tagged FBP2 or FLAG-expressing plasmid, and the dicistronic plasmid was then transfected into cells after 48 h post-transfection. Cell lyastes were also collected and analyzed to determine RLuc and FLuc activity after 48 h post-transfection. Over-expression of FBP2/FLAG reduced the EV71 IRES activity to 74% ($P < 0.05$) (Figure 6A, right). The lower panel of Figure 6A shows the over-expression efficiency of FBP2.

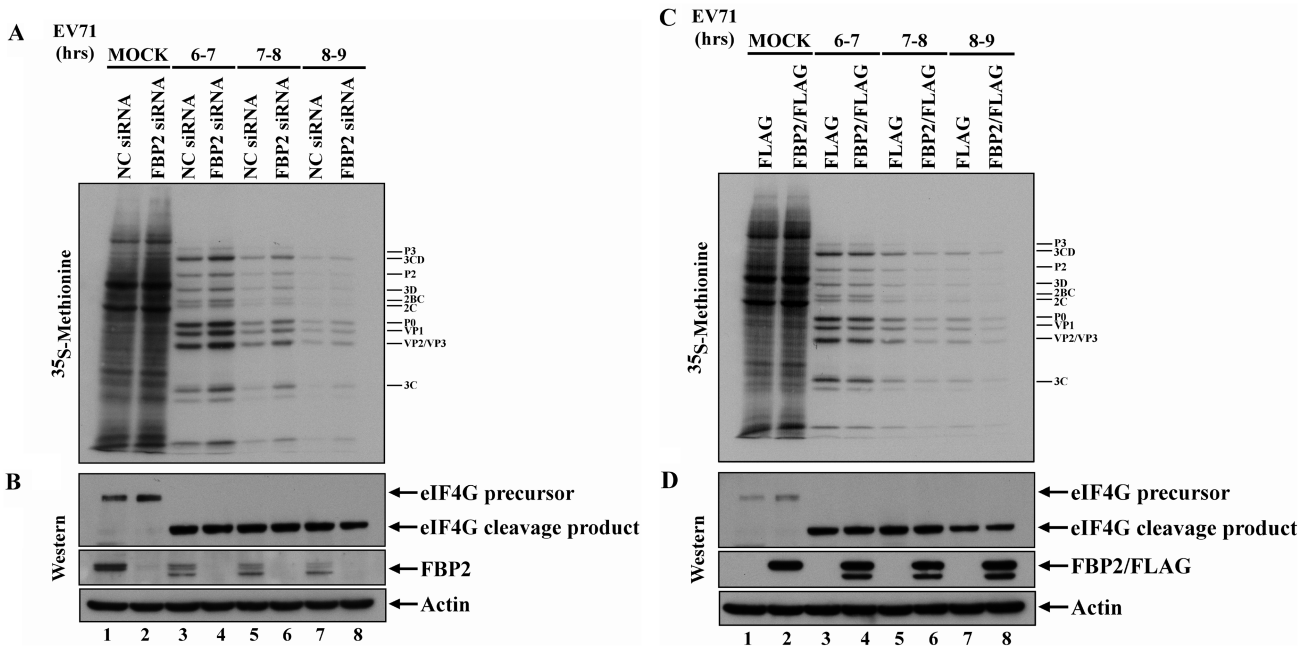

Figure 5. FBP2 regulates EV71 viral protein synthesis. (**A**) Transfection of siRNA [negative control siRNA (NC siRNA), or siRNA against FBP2 (FBP2 siRNA)] in RD cells was performed in 12-well plates. Following transfection, cells were infected with EV71 or mock-infected, and protein synthesis was examined by pulse-labeling at various times, as described in Materials and methods section. (**B**) Western blot analysis of FBP2 protein. (**C**) Transfection of FLAG or FBP2/FLAG plasmid DNA in RD cells was performed in 12-well plates. Following transfection, cells were infected with EV71 or mock-infected, and protein synthesis was examined by pulse-labeling at various times, as described in Materials and methods section. (**D**) Western blot analysis of FBP2/FLAG protein.

The direct transfection of dicistronic reporter mRNA was performed. Figure 6B indicates that EV71 IRES activity is increased to 111% ($P < 0.05$) in FBP2-knockdown cells and reduced to 90% ($P < 0.001$) in FBP2-overepressed cells. The FLuc/RLuc ratio following DNA transfection may be related to a nuclear event, such as the use of a cryptic promoter or the splice site in the IRES sequence. Accordingly, monocistronic mRNAs that contained the EV71 5′ UTR were alternatively transfected into RD cells, and the FLuc activity was measured after RD cells were transfected by FBP2 siRNA (knock-down) or FBP2/FLAG (over-expression). The knockdown of endogenous FBP2 protein increased EV71 IRES activity to 132% ($P < 0.05$) of that of the NC control (Figure 6C, left). The lower panel of Figure 6C displays the knockdown efficiency of FBP2. RD cells were transiently transfected with a FLAG-tagged FBP2 or FLAG-expressing plasmid, and then the monocistronic mRNA was transfected into cells after 48-h post-transfection. Cell lyastes were also collected and analyzed to determine FLuc activity after 6 h post-transfection. The over-expression of FBP2/FLAG reduced EV71 IRES activity to 57% ($P < 0.05$) (Figure 6C, right). These results together indicate that FBP2 may act as a negative regulator of EV71 IRES function.

Mechanism of negative regulation by FBP2

Two hypotheses seek to explain how FBP2 serves as a negative regulator of EV71 IRES. First, FBP2 is an important adenosine-uridine element binding protein (ARE-BP) that is known to influence RNA stability. In this work, the viral RNA integrity was further investigated in FBP2 knocked-down cells. The right panel of Figure 7A reveals that FBP2 was knocked down by its specific siRNA. 40 MOI of EV71 was used to infect cells and viral RNAs were extracted at various times post-infection. Slot-blot assay using a specific RNA probe against either positive or negative sense EV71 viral RNA was employed to monitor viral RNA synthesis. The results in Figure 7A indicate that neither positive nor negative stranded EV71 RNA in FBP2 siRNA-treated cells differed from that in NC siRNA-treated cells.

Another hypothesis is that FBP2 competes with other positive ITAFs to bind with specific EV71 IRES and thereby negatively regulate IRES activity. *In vitro* competition binding assay was performed. Various amounts of recombinant PTB protein, a positive ITAF of picornavirus, were added to the *in vitro* binding assay and the results show that FBP2 outcompeted PTB for IRES binding (Figure 7B). Taken together, these results support the second hypothesis—that FBP2 may compete with EV71 positive ITAFs, so that FBP2 acts as negative regulator.

DISCUSSION

An internal ribosomal entry site (IRES) that directs the initiation of viral protein translation is a potential drug target for enterovirus 71 (EV71). This investigation identified the trans-acting factors associated with EV71 5′ UTR to elucidate the mechanism of the initiation of

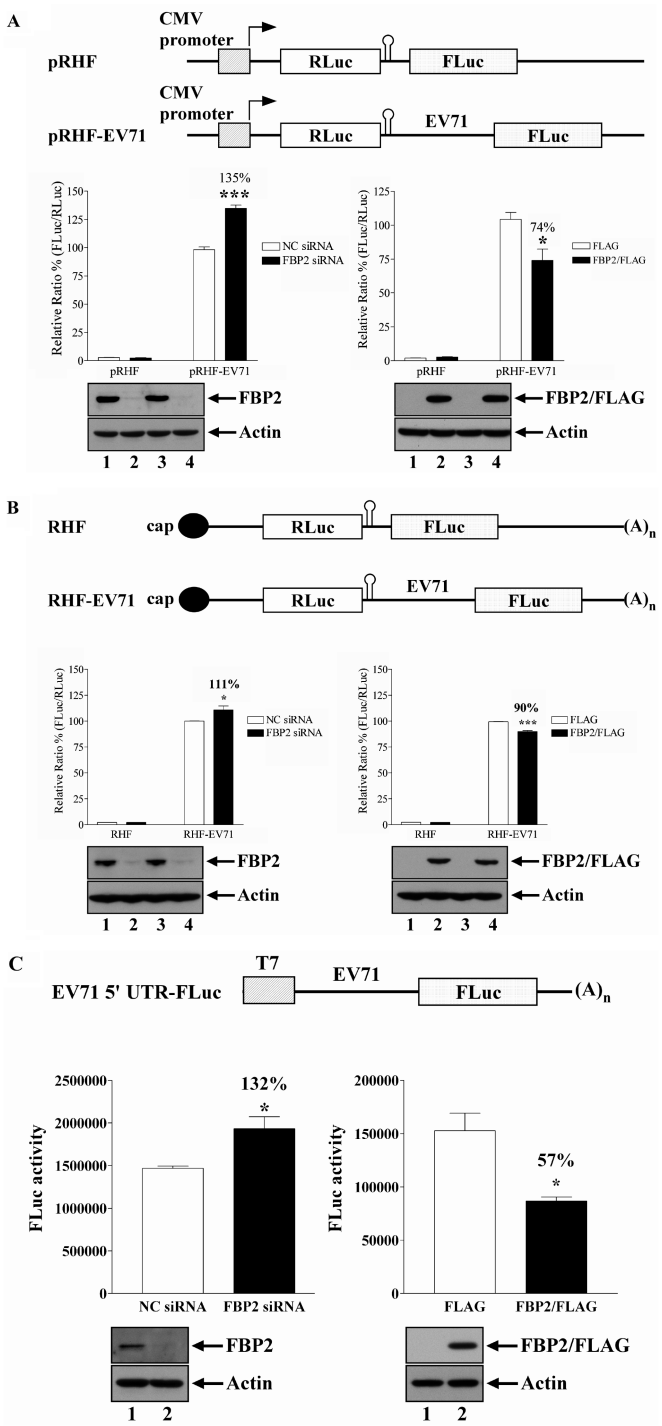

Figure 6. Effects of down-regulation and up-regulation of FBP2 on EV71 IRES activity. (**A**) Schematic diagram of dicistronic reporter plasmids pRHF and pRHF–EV71-5′UTR. Plasmid expresses dicistronic mRNA, consisting of the Renilla luciferase (RLuc) gene at the first cistron and the EV71-5′ UTR and the Firefly luciferase (FLuc) gene at the second cistron (CMV, cytomegalovirus). A hairpin (H) is inserted downstream of the first cistron to prevent ribosome read-through. RD cells were firstly transfected with either FBP2 siRNA or pFBP2/FLAG. After 3 days, dicistronic construct pRHF or pRHF–EV71-5′UTR and siRNA duplexes were cotransfected into RD cells with siRNA duplex. At 48-h post-cotransfection, the Renilla luciferase (RLuc) and Firefly luciferase (FLuc) activity in cell lysates were analyzed. The bars in the histogram represent FLuc/RLuc activity percentages. Experiments were performed in triplicate to obtain the bar graph. Western blotting was utilized analyze the expression levels of FBP2, FBP2/FLAG and actin. (**B**) Schematic diagram of capped dicistronic mRNAs containing a poly(A) tail. RD cells transfected with either FBP2 siRNA or FBP2/FLAG were grown for 3 days and then transfected with RHF or RHF-EV71-5′ UTR. After 6-h post-transfection, cells were harvested, lysed and western blotted for FBP2, FBP2/FLAG and actin. An aliquot of the lysate was assayed for Renilla luciferase and Firefly luciferase (FLuc) activity. (**C**) Schematic diagram of monocistronic reporter plasmids EV71 5′ UTR-FLuc. RD cells transfected with either FBP2 siRNA or FBP2/FLAG were grown for 3 days and then transfected with EV71 5′ UTR-FLuc mRNA. After 6-h post-transfection, cells were harvested, lysed and western blotted for FBP2, FBP2/FLAG and actin. An aliquot of the lysate was assayed for Firefly luciferase (FLuc) activity. ($^{*}P < 0.05$ and $^{***}P < 0.001$, Student's two-tailed unpaired *t*-test).

translation on EV71. In the past, the most commonly employed experimental strategy involved either UV cross-linking or electrophoretic mobility-shift assays to identify proteins that interact with picornavirus 5′ UTR. However, this work utilizes a biotinylated RNA-protein pull-down assay, combined with MALDI-TOF analysis, to provide a global view of cellular proteins that associate with EV71 5′ UTR.

IRES-specific trans-acting factors (ITAFs) that are involved in the functionality of the EV71 IRES are sought and far upstream element binding 2 (FBP2) is identified as a novel EV71 IRES ITAFs. FBP2 is also known as KH-type splicing regulatory protein (KSRP). It is originally identified as a component of a protein complex that assembles on an intronic c-src neuronal-specific splicing enhancer, is an important adenosine-uridine element binding protein (ARE-BP) that is known to interact with several AREs (22,23).

This study is first to report that FBP2 binds to the highly structured EV71 5′ UTR. This fact is demonstrated by RNA affinity capture experiments. It demonstrates that the binding of FBP2 to EV71 5′ UTR is specific. Its binding to biotinylated EV71 5′ UTR is not competitively eliminated by non-specific RNA, such as yeast tRNA (Figure 1B, lanes 8–10), but is competitively eliminated by cold non-biotinylated EV71 5′ UTR in a concentration-dependent manner (Figure 1B, lanes 3–5). Since FBP2 proteins mostly accumulate in the nuclear compartment (24), an important question is how a nucleus-localized host protein interacts with EV71 RNA in the cytoplasm and modulates viral replication. Immunofluorescence experiments have indicated that a significant portion of FBP2 is present in the cytoplasm after EV71 infection (Figure 4A), where it can interact with EV71 RNA. Co-immunoprecipitation assay is also employed to demonstrate that FBP2 associates with EV71 5′ UTR in EV71-infected cells (Figure 4B).

A single-cycle virus replication assay was conducted in FBP2-knockdown and FBP2-overexpressed cells. Viral yields decreased slightly by less than order of magnitude in FBP2-overexpressed cells, but did not visibly observably differ in FBP2-knockdown cells. FBP2 seemingly modulates viral protein synthesis (Figure 5), but whether FBP2 influences any other cellular process during EV71 infection is unclear. The effect of FBP2 on cellular machinery

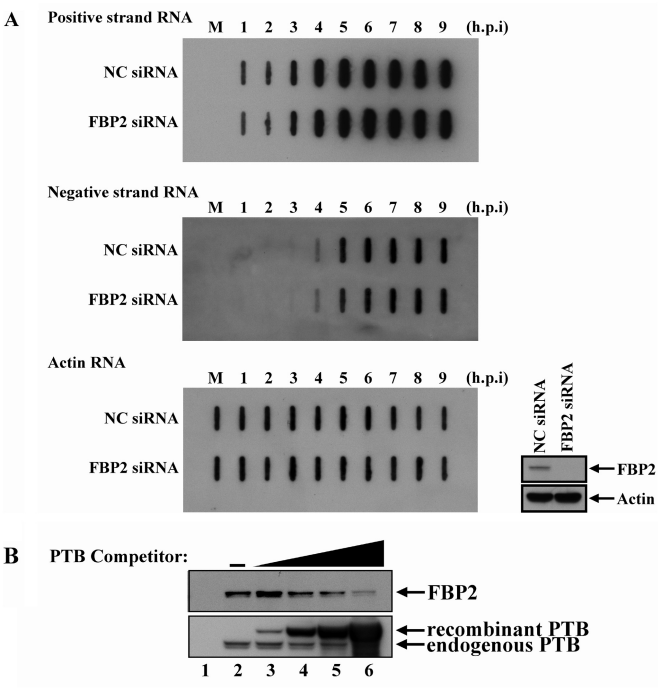

Figure 7. Mechanism of negative regulation by FBP2. (**A**) Viral RNA synthesis was not affected in FBP2 knock-down cells. After RD cells had been transfected with FBP2 and NC siRNA for 48-h, the cells were reseeded into plates. 24-h thereafter, the cells were infected with EV71 (4643/TW/1998) at 40 MOI and RNA was extracted at various times post-infection. RNA was loaded onto a nitrocellulose sheet in the slot-blot manifold. After washing, it was air-dried and crosslinked, and the nitrocellulose was prehybridized. DIG-labeled RNA probes, specific for either the genome or the antigenome were added and incubated. Following washing and blocking, the blots were incubated with chemi-luminescent substrate for visualization. (**B**) FBP2 was outcompeted by PTB recombinant protein for IRES binding. The pull-down assay that was displayed in Figure 1A was performed here. The eluted proteins were subjected to SDS–PAGE (12%). Antibodies against FBP2 and PTB were utilized in western blot analysis. Various amounts of PTB recombinant protein were added to compete with FBP2 in interacting with biotin-labeled EV71 5′ UTR. In the negative control, non-biotinylated RNA was added to the reaction in lane 1. PTB competitor was used in the competition assay (lanes 3–6).

may reduce viral yields in FBP2 knockdown cells, which then exhibited no observable difference in viral titer when a single-cycle virus was replicated in FBP2-knockdown cells in which viral yields were expected to be increased.

The viral components i.e. viral RNA and viral proteins are made in great excess under normal condition in infected cells. Therefore several fold fluctuation in the amounts of viral proteins would not be expected to reflect in virus yield. As the amounts of viral proteins are surplus in untreated cells, the 'extra' amounts of viral proteins (~2-fold) made in FBP 2-depleted cells would not dramatically increase the virus yield. Similarly, the decreased synthesis of viral proteins (~2-fold) resulted from over-expression of FBP2 would not significantly decrease the virus yield. We therefore would like to emphasize the effect of FBP 2 is mainly on the viral protein synthesis, i.e. the IRES-dependent translation. The growth rate of EV71 was found slower than that of other enteroviruses (PV, CB3, etc). We have performed 'one-step' growth rate analysis and noticed that the viral titer usually peaks and reaches plateau at 12–15 h (data not shown). We also performed extensive time course experiments to monitor the viral translation, and found little viral protein synthesis at early time points by metabolic radiolabeling experiment. As a result the effect of FBP2 on viral protein synthesis was hardly evaluated prior to 6-h post-infection (Figure 5).

Many other proteins that are primarily localized in the nucleus also interact with picornaviral RNA in the cytoplasm. Various nuclear localization cellular factors, such as PTB (25), hnRNP C (26), hnRNP K (27), hnRNP A1 (28) and nuclear factors (NF45) (29), interact with picornaviral RNA and affect picornaviral replication and/or translation. The interaction between the nucleus-localized host cellular factors and EV71 RNA provides two important pieces of information for viral-host interactions on EV71 infection. First, EV71 infection may influence the cellular distribution of numerous host proteins, such as hnRNP A1, hnRNP K and hnRNP C (27,30) and the nuclear factors (NF45) (29). Second, some of these host proteins, such as PTB (25), hnRNP C (26) and the nuclear factors (NF45) (29), may have important, active functions in the viral life cycle.

Why did FBP2 relocalize to cytoplasm—because EV71 RNA simply tethers FBP2 in the cytoplasm or because EV71 infection influences the nuclear-cytoplasmic transport of FBP2? The localization of FBP2 in EV71 IRES reporter construct-transfected cells was examined. FBP2 remained localized in the nuclei of transfected cells (Figure S1 in the Supplementary Data). The results suggest that EV71 infection but not IRES alone caused the relocalization of FBP2, which also highlights the modest effect of FBP2 knockdown on the EV71 IRES reporter constructs (Figure 6). Therefore, EV71 IRES activity was measured again with co-infection with EV71. Figure S2 in the Supplementary Data presents the results. After 2 h post-infection, monocistronic mRNA that contains EV71 IRES and FLuc as a reporter was transfected into cells. Cell lysates were collected and analyzed to determine FLuc activity after 4 h post-transfection. The results indicate that EV71 infection increased the effect of FBP2 on EV71 IRES activity by a factor of ~1.2 times over that of mock-infection.

Two speculated hypotheses seek to explain how FBP2 serves as a negative regulator of EV71 IRES. First, FBP2 is an important ARE-BP that is known to interact with many AREs. The central part of the protein is organized in four K-homology domains. The KH4 domain of FBP2 is essential for mRNA decay and ARE recognition, and its deletion results in the complete loss of these activities (31,32). FBP2 interacts with the AU-rich elements that destabilize *fos* mRNA and with the human exosome complex *in vitro*. Depletion/addback experiments in a cytoplasmic *in vitro* degradation system support a role for the protein involvement in targeting mRNAs for degradation (23). The interaction between FBP2 and EV71 5′ UTR was verified by mapping the interaction regions to nt 1–167, 91–228 and 566–745 in EV71 5′ UTR and KH2 and KH4 domains in FBP2 (Figures 2B and 3B). FBP2 may inhibit EV71 IRES because the binding of

FBP2 to EV71 5′ UTR may destroy the structure of IRES and therefore degrades the viral RNA. Second, some cellular proteins identified from MALDI-TOF in Table 1 were mapped as having the binding sites in EV71 5′ UTR that overlap with that of FBP2. Such proteins are PTB, hnRNP A1 and FBP (data not shown). This finding raises one possibility that FBP2 may compete with other ITAFs to bind with specific EV71 IRES and thereby regulate IRES activity in a negative manner. An *in vitro* competition binding assay was performed and the results in Figure 7B reveal that FBP2 outcompeted the binding of PTB. PTB has been demonstrated to be a positive ITAF for other picornaviruses (20,33). The result suggests that FBP2 may compete with other ITAFs to act as a negative regulator of EV71 IRES.

The FLuc/RLuc ratio following DNA transfection may also be related to a nuclear event, such as the use of a cryptic promoter or the use of a splicing site in the IRES sequence. Accordingly, monocistronic mRNA was utilized to measure EV71 IRES activity. The results of EV71 IRES activity were consistent with that of a dicistronic construct. All of the results reveal that the knocking down of FBP2 expression increase EV71 IRES activity, while the up-regulation of FBP2 expression reduced EV71 IRES activity (Figure 6A, B and C). The sequence of the construct was examined and no splicing site was present within EV71 IRES. RT-PCR was also performed to confirm the absence of a splicing product of EV71 IRES RNA (Figure S3).

To our knowledge, this investigation is the first to describe on the molecular level negative regulation by FBP2 of EV71 translation. These studies help not only to understand the function of IRES but also further investigations of the mechanism by which cellular proteins are involved in EV71 infection.

SUPPLEMENTARY DATA

Supplementary Data are available at NAR Online.

ACKNOWLEDGEMENTS

The authors would like to thank the Proteomic Center of Chang Gung University, and especially Dr Jau-Song Yu, for technical support. Ted Knoy is appreciated for his editorial assistance. Special thanks to Dr Roberto Gherzi for providing the pCMV-Tag2B-KSRP plasmid.

FUNDING

National Science Council of Taiwan, the Republic of China (NSC-94-3112-B-182-006). Funding for open access charge: Research Program for Chang Gung Memorial Hospital (BMRP 367), Taoyuan, Taiwan.

Conflict of interest statement. None declared.

REFERENCES

1. McMinn,P.C. (2002) An overview of the evolution of enterovirus 71 and its clinical and public health significance. *FEMS Microbiol. Rev*., **26**, 91–107.
2. AbuBakar,S., Chee,H.Y., Al-Kobaisi,M.F., Xiaoshan,J., Chua,K.B. and Lam,S.K. (1999) Identification of enterovirus 71 isolates from an outbreak of hand, foot and mouth disease (HFMD) with fatal cases of encephalomyelitis in Malaysia. *Virus Res*., **61**, 1–9.
3. Alexander,J.P. Jr, Baden,L., Pallansch,M.A. and Anderson,L.J. (1994) Enterovirus 71 infections and neurologic disease–United States, 1977–1991. *J. Infect. Dis*., **169**, 905–908.
4. Gilbert,G.L., Dickson,K.E., Waters,M.J., Kennett,M.L., Land,S.A. and Sneddon,M. (1988) Outbreak of enterovirus 71 infection in Victoria, Australia, with a high incidence of neurologic involvement. *Pediatr. Infect. Dis. J*., **7**, 484–488.
5. Ho,M., Chen,E.R., Hsu,K.H., Twu,S.J., Chen,K.T., Tsai,S.F., Wang,J.R. and Shih,S.R. (1999) An epidemic of enterovirus 71 infection in Taiwan. Taiwan Enterovirus Epidemic Working Group. *N. Engl. J. Med*., **341**, 929–935.
6. Kehle,J., Roth,B., Metzger,C., Pfitzner,A. and Enders,G. (2003) Molecular characterization of an Enterovirus 71 causing neurological disease in Germany. *J. Neurovirol*., **9**, 126–128.
7. McMinn,P., Lindsay,K., Perera,D., Chan,H.M., Chan,K.P. and Cardosa,M.J. (2001) Phylogenetic analysis of enterovirus 71 strains isolated during linked epidemics in Malaysia, Singapore, and Western Australia. *J. Virol*., **75**, 7732–7738.
8. Zhang,S.B., Liao,H., Huang,C.H., Tan,Q.Y., Zhang,W.L., Huang,Y., Chen,K., Qiu,S.Q., Xing,S.Z. and Liao,Y.H. (2008) [Serum types of enterovirus and clinical characteristics of 237 children with hand, foot and mouth disease in Shenzhen]. *Zhongguo dang dai er ke za zhi = Chinese J. Contempor. Pediatr*., **10**, 38–41.
9. Haghighat,A., Svitkin,Y., Novoa,I., Kuechler,E., Skern,T. and Sonenberg,N. (1996) The eIF4G-eIF4E complex is the target for direct cleavage by the rhinovirus 2A proteinase. *J. Virol*., **70**, 8444–8450.
10. Joachims,M., Van Breugel,P.C. and Lloyd,R.E. (1999) Cleavage of poly(A)-binding protein by enterovirus proteases concurrent with inhibition of translation in vitro. *J. Virol*., **73**, 718–727.
11. Krausslich,H.G., Nicklin,M.J., Toyoda,H., Etchison,D. and Wimmer,E. (1987) Poliovirus proteinase 2A induces cleavage of eucaryotic initiation factor 4F polypeptide p220. *J. Virol*., **61**, 2711–2718.
12. Thompson,S.R. and Sarnow,P. (2003) Enterovirus 71 contains a type I IRES element that functions when eukaryotic initiation factor eIF4G is cleaved. *Virology*, **315**, 259–266.
13. Pilipenko,E.V., Pestova,T.V., Kolupaeva,V.G., Khitrina,E.V., Poperechnaya,A.N., Agol,V.I. and Hellen,C.U. (2000) A cell cycle-dependent protein serves as a template-specific translation initiation factor. *Genes. Dev*., **14**, 2028–2045.
14. Blyn,L.B., Towner,J.S., Semler,B.L. and Ehrenfeld,E. (1997) Requirement of poly(rC) binding protein 2 for translation of poliovirus RNA. *J. Virol*., **71**, 6243–6246.
15. Boussadia,O., Niepmann,M., Creancier,L., Prats,A.C., Dautry,F. and Jacquemin-Sablon,H. (2003) Unr is required in vivo for efficient initiation of translation from the internal ribosome entry sites of both rhinovirus and poliovirus. *J. Virol*., **77**, 3353–3359.
16. Costa-Mattioli,M., Svitkin,Y. and Sonenberg,N. (2004) La autoantigen is necessary for optimal function of the poliovirus and hepatitis C virus internal ribosome entry site in vivo and in vitro. *Mol. Cell. Biol*., **24**, 6861–6870.
17. Lee,J.C., Wu,T.Y., Huang,C.F., Yang,F.M., Shih,S.R. and Hsu,J.T. (2005) High-efficiency protein expression mediated by enterovirus 71 internal ribosome entry site. *Biotechnol.Bioeng*., **90**, 656–662.
18. Walter,B.L., Parsley,T.B., Ehrenfeld,E. and Semler,B.L. (2002) Distinct poly(rC) binding protein KH domain determinants for poliovirus translation initiation and viral RNA replication. *J. Virol*., **76**, 12008–12022.
19. Walter,B.L., Nguyen,J.H., Ehrenfeld,E. and Semler,B.L. (1999) Differential utilization of poly(rC) binding protein 2 in translation directed by picornavirus IRES elements. *RNA*, **5**, 1570–1585.
20. Hellen,C.U., Witherell,G.W., Schmid,M., Shin,S.H., Pestova,T.V., Gil,A. and Wimmer,E. (1993) A cytoplasmic 57-kDa protein that is required for translation of picornavirus RNA by internal ribosomal entry is identical to the nuclear pyrimidine tract-binding protein. *Proc. Natl Acad. Sci. USA*, **90**, 7642–7646.
21. Shih,S.R., Chiang,C., Chen,T.C., Wu,C.N., Hsu,J.T., Lee,J.C., Hwang,M.J., Li,M.L., Chen,G.W. and Ho,M.S. (2004) Mutations at KFRDI and VGK domains of enterovirus 71 3C protease affect

its RNA binding and proteolytic activities. *J. Biomed. Sci.*, **11**, 239–248.
22. Min,H., Turck,C.W., Nikolic,J.M. and Black,D.L. (1997) A new regulatory protein, KSRP, mediates exon inclusion through an intronic splicing enhancer. *Genes. Dev.*, **11**, 1023–1036.
23. Chen,C.Y., Gherzi,R., Ong,S.E., Chan,E.L., Raijmakers,R., Pruijn,G.J., Stoecklin,G., Moroni,C., Mann,M. and Karin,M. (2001) AU binding proteins recruit the exosome to degrade ARE-containing mRNAs. *Cell*, **107**, 451–464.
24. He,L., Weber,A. and Levens,D. (2000) Nuclear targeting determinants of the far upstream element binding protein,a c-myc transcription factor. *Nucleic Acids Res.*, **28**, 4558–4565.
25. Song,Y., Tzima,E., Ochs,K., Bassili,G., Trusheim,H., Linder,M., Preissner,K.T. and Niepmann,M. (2005) Evidence for an RNA chaperone function of polypyrimidine tract-binding protein in picornavirus translation. *RNA*, **11**, 1809–1824.
26. Brunner,J.E., Nguyen,J.H., Roehl,H.H., Ho,T.V., Swiderek,K.M. and Semler,B.L. (2005) Functional interaction of heterogeneous nuclear ribonucleoprotein C with poliovirus RNA synthesis initiation complexes. *J. Virol.*, **79**, 3254–3266.
27. Lin,J.Y., Li,M.L., Huang,P.N., Chien,K.Y., Horng,J.T. and Shih,S.R. (2008) Heterogeneous nuclear ribonuclear protein K interacts with the enterovirus 71 5′ untranslated region and participates in virus replication. *J. Gen. Virol.*, **89**, 2540–2549.
28. Cammas,A., Pileur,F., Bonnal,S., Lewis,S.M., Leveque,N., Holcik,M. and Vagner,S. (2007) Cytoplasmic relocalization of heterogeneous nuclear ribonucleoprotein A1 controls translation initiation of specific mRNAs. *Mol. Biol. Cell*, **18**, 5048–5059.
29. Merrill,M.K. and Gromeier,M. (2006) The double-stranded RNA binding protein 76:NF45 heterodimer inhibits translation initiation at the rhinovirus type 2 internal ribosome entry site. *J. Virol.*, **80**, 6936–6942.
30. Gustin,K.E. and Sarnow,P. (2001) Effects of poliovirus infection on nucleo-cytoplasmic trafficking and nuclear pore complex composition. *EMBO J.*, **20**, 240–249.
31. Gherzi,R., Lee,K.Y., Briata,P., Wegmuller,D., Moroni,C., Karin,M. and Chen,C.Y. (2004) A KH domain RNA binding protein, KSRP, promotes ARE-directed mRNA turnover by recruiting the degradation machinery. *Mol. Cell*, **14**, 571–583.
32. Garcia-Mayoral,M.F., Hollingworth,D., Masino,L., Diaz-Moreno,I., Kelly,G., Gherzi,R., Chou,C.F., Chen,C.Y. and Ramos,A. (2007) The structure of the C-terminal KH domains of KSRP reveals a noncanonical motif important for mRNA degradation. *Structure*, **15**, 485–498.
33. Hellen,C.U., Pestova,T.V., Litterst,M. and Wimmer,E. (1994) The cellular polypeptide p57 (pyrimidine tract-binding protein) binds to multiple sites in the poliovirus 5′ nontranslated region. *J. Virol.*, **68**, 941–950.